



Insights into sorption and molecular transport of atrazine, testosterone, and progesterone onto polyamide microplastics in different aquatic matrices

Mariana A. Dias^{a,*}, Patrick R. Batista^b, Lucas C. Ducati^b, Cassiana C. Montagner^a

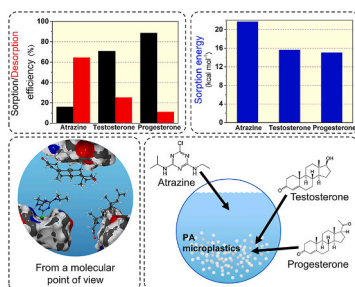
^a Environmental Chemistry Laboratory, Institute of Chemistry, University of Campinas, Campinas, São Paulo, 13083970, Brazil

^b Department of Fundamental Chemistry, Institute of Chemistry, University of São Paulo, São Paulo, 05508000, Brazil

HIGHLIGHTS

- Polyamide microplastics present a high sorption efficiency for progesterone.
- Physicochemical properties of the water systems influence the sorption capacity.
- The experimental and theoretical results agree with the sorption order.
- Hydrogen bonds and electrostatic interactions occur in the microplastic complexes.

GRAPHICAL ABSTRACT



ARTICLE INFO

Handling Editor: Carlos Alberto Martínez-Huitle

Keywords:
Pesticide
Hormone
Kinetic
Isotherm
Molecular dynamics
Density functional theory.

ABSTRACT

Microplastics can act as vectors of a wide class of contaminants in aquatic environments. The sorption behavior of two hormones known to cause adverse effects in biota even in low concentrations (testosterone-TTR and progesterone-PGT), and a pesticide with a high environmental persistence known as endocrine disruptor chemical (atrazine-ATZ) onto polyamide (PA) microplastics is investigated under different aquatic matrices using kinetic and isotherm experiments. The sorption equilibrium is achieved in 48 h, and the experimental results are better fitted by pseudo-2nd-order model. Langmuir isotherm better describes the sorption of the contaminants onto PA microplastics. PGT presents the highest sorption efficiency at around 90%, followed by TTR at 70% and ATZ at approximately 20%. Moreover, ATZ is the contaminant with the highest desorption efficiency (~65%), indicating its preference for staying solubilized in water. Combining classical molecular dynamics and density functional theory calculations, the sorption energies were calculated as 12–15 kcal mol⁻¹, 13–16 kcal mol⁻¹, and 19–22 kcal mol⁻¹ for PGT, TTR, and ATZ, respectively, showing that PGT needs less energy to be transferred from the solvent network to the PA surface, in agreement with experimental results. The sorption mechanism is driven by hydrogen bonds onto PA outer surface, while the electrostatic interactions dominate the PA inner surface sorption. Moreover, the sorption efficiency is statistically different between the investigated matrices, indicating that physicochemical characteristics of water systems could influence the interactions between PA-contaminant. In seawater, the phenomena of salting-out/in and competitive sorption with saline ions are observed for three contaminants. The PA-contaminant complexes are more polar and soluble than the dissociated ones, which increases the contaminant's co-transport by PA in water.

* Corresponding author.

E-mail address: m230015@dac.unicamp.br (M.A. Dias).

<https://doi.org/10.1016/j.chemosphere.2023.137949>

Received 27 October 2022; Received in revised form 16 January 2023; Accepted 22 January 2023

Available online 26 January 2023

0045-6535/© 2023 Elsevier Ltd. All rights reserved.

1. Introduction

Microplastics (plastic particles with sizes between 1 μm and 1000 μm) (ISO, 2020), defined as emerging contaminants (Richardson and Kimura, 2016), have been an environmental concern due to their occurrence in all compartments, such as air, soil, and aquatic systems (Montagner et al., 2021). Therefore, microplastics have acted as potential transport vectors of chemicals, both inorganics (e.g., metals) and organics (e.g., pharmaceuticals, hormones, pesticides, and industrial chemicals, referred to as contaminants from here) (Caruso, 2019). Some contaminants could leach from microplastics (Li et al., 2021), especially additives used in plastic manufacture, or could migrate from the environment to the microplastics. Thus, plastic particles are no longer only a physical problem in the environment but also a chemical issue.

Fibers from synthetic fabrics have been one of the main sources of microplastics in the environment due to their discharge into water systems through laundry (Herzke et al., 2021). These fibers are mainly composed of polar polymers like polyamide (PA) (de Falco et al., 2019). Once in the environment, textile fibers are subject to degradative processes influenced by UV light exposure, biodegradation, hydrolysis, and mechanical abrasion. Thus, the fibers could break into smaller pieces and change their morphology, originating fragments. Sait et al. (2021) showed that PA fibers could degrade, reaching nano-sized particles.

Unlike non-polar polymers, exclusively composed of hydrogen and carbon atoms, the inclusion of polar groups on the polymer structure, such as amide, could potentialize the chemical interactions with environmental contaminants through hydrogen bonds (Torres et al., 2021). For instance, Lara et al. (2021) obtained high sorption efficiency, ranging from 56% to 90%, in laboratory studies involving PA microplastics and hormones under different simulated environmental conditions. In addition, PA also presented higher affinities with pharmaceuticals than other polymers as reported by Guo et al. (2019a, 2019b) and Li et al. (2018), and it has also exhibited considerable sorption of petroleum hydrocarbons (Seidensticker et al., 2019; Song et al., 2021), perfluorooctanoic and perfluorooctanesulphonic acids (Ateia et al., 2020).

Pesticides including atrazine (ATZ) and hormones, such as progesterone (PGT) and testosterone (TTR) have been frequently found in the aquatic environment and, therefore, are of great concern. ATZ is a pre- and post-emergent triazine herbicide used in various crops. Thus, ATZ has been one of the best-selling pesticides around the world. Although its use has been banned in the European Union since 2003, it continues to be widely used in other countries, such as the United States, China, and Brazil. In 2020, ATZ ranked fourth in the Brazilian ranking of pesticide commercialization, with more than 33,000 tons of active ingredient sold (IBAMA, 2020), representing almost half of world production (Sadeghnia et al., 2021). ATZ is ubiquitous owing to its persistence, especially in aquatic matrices (Montagner et al., 2018; Stefano et al., 2022) and even in the atmosphere (Alonso et al., 2018; Dias et al., 2021). Some adverse effects on aquatic biota have been related to ATZ exposure. In the same way, in humans, ATZ could disrupt the endocrine system, damage the cardiovascular, reproductive, and gastric systems, and cause cancer (Sadeghnia et al., 2021).

Steroid hormones (PGT and TTR) are also classified as emerging contaminants (Richardson and Ternes, 2022) and have been reported in aquatic compartments around the world. Their input into the environment originates from untreated sewage discharge in water bodies or inefficient water treatment. It has been shown that very low concentrations of these hormones, in the order of few ng L^{-1} , can cause adverse effects on biota due to their acting as endocrine disrupting chemicals (EDC) (Adeel et al., 2017; Siri et al., 2021; Sousa et al., 2018). Thus, the biota can be exposed to these EDCs either via contaminants solubilized in water or via contaminants sorbed to microplastics. For instance, Guedes-Alonso et al. (2021) quantified PGT and TTR sorbed to microplastics collected on beaches of the Canary Islands at concentrations from 9.1 ng g^{-1} to 26.1 ng g^{-1} and 15.0 ng g^{-1} to 37.3 ng g^{-1} ,

respectively.

Therefore, as aforementioned ATZ and hormones (see Table S1 for more information) require special attention due to their occurrence in the aquatic matrices allowing interactions with microplastics. Nonetheless, up to date, we have found no studies dedicated to the sorption of these contaminants onto PA-Nylon 6 (referred to as PA from here) microplastics, which is a commonly used textile polymer. The main goal of this study is to address this issue through sorption experiments and employing classical molecular dynamics (MD) and density functional theory (DFT) calculations. Additionally, the behavior of the three contaminants is assessed under different aquatic matrices, ultrapure water (UW), groundwater (GW), surface water (SFW), and seawater (SW). Finally, the sorption energy and the main PA-contaminant interactions are obtained and discussed in the molecular approach.

2. Materials and methods

2.1. Materials

High purity standards of ATZ (99.11%, CAS #1912-24-9), TTR (99%, CAS #58-22-0), and PGT (98%, CAS #57-83-0) were purchased from Merck (Darmstadt, Germany). Stock solutions of each contaminant were prepared in methanol at concentrations of approximately 300–500 mg L^{-1} , and the working solutions were prepared by diluting the stock solution in water. HPLC-grade methanol and formic acid were obtained from Merck. Ultrapure water was obtained from a Synergy Water Purification System from Millipore (Burlington, USA). PA pellets (Nylon 6 – Domamid H24) were acquired from DOMO Chemicals (Ghent, Belgium) and milled in an analytical mill (Marconi MA 580, Brazil) obtaining microplastics with particle size smaller than 106 μm .

2.2. Polyamide microplastic characterization

The morphologies of the samples were examined with a Quanta 250 field emission scanning electron microscope (SEM) (FEI Co., USA). The functional groups of PA microplastics were characterized using Fourier transform infrared spectroscopy (FTIR, Agilent, Cary 630) with the attenuated total reflection (ATR) technique.

2.3. Sampling and physicochemical characterization of water samples

The sorption studies were performed using ultrapure water (UW) and three real environmental water samples. Groundwater (GW) was sampled at the source of Ribeirão das Pedras creek (22°51'43.9"S 47°03'24.8"W, Campinas, São Paulo, Brazil), surface water (SFW) was collected at the Atibaia River (22°52'41.7"S 46°57'56.5"W, Campinas, São Paulo, Brazil), and seawater (SW) was obtained from Guarujá beach (23°59'10.8"S 46°13'13.6"W, Guarujá, São Paulo, Brazil). All samples were collected in 1-L amber glass bottles, previously decontaminated with ultrapure water, ethanol, and acetone, followed by calcination at 400 °C for 4 h.

Conductivity (Digimed DM-32, Brazil) and pH (Digimed DM-22) parameters were measured immediately after sampling. Water samples were vacuum-filtered using a glass microfiber membrane (47 mm diameter, grade 13,400) from Sartorius (Göttingen, Germany). ATZ, PGT, and TTR concentrations in water samples were determined using solid-phase extraction followed by liquid chromatography coupled to mass spectrometry in tandem (LC-MS/MS) analysis, according to a method previously validated by our research group (Montagner et al., 2014). Instrumental limits of detection (LOD) and quantification (LOQ) were obtained using 3-fold and 10-fold signal-to-noise ratios, respectively. These values are shown in Table S3.

2.4. Batch sorption experiments

In the sorption experiments, 20 mg of PA microplastics and 2.0 mL of

contaminant solution (ATZ, PGT, and TTR) were added to glass tubes (10 mL) capped with polytetrafluoroethylene (PTFE) caps and placed on a roto torque shaker (Marconi MA161/ROTO) at room temperature (20 °C) and 80 rpm. Kinetic experiments were conducted with a fixed initial contaminant concentration of 1.0 mg L⁻¹. The contaminants concentrations in the liquid phase were assessed at 0.5, 1, 2, 3, 6, 12, 24, 48, 72, 96, and 108 h. Sorption isotherm experiments were performed with initial contaminant concentrations set as 0.01, 0.05, 0.1, 0.2, 0.5, 1.0, and 2.0 mg L⁻¹. All experiments were performed in triplicate. Before analyses, the samples were kept at rest for approximately 5 min to allow the microplastics to settle. The supernatant was filtered through 0.22 µm PTFE syringe filters and diluted for LC-MS/MS analysis. The sample preparation and chemical analysis were performed according to the procedures described in the [Supporting Information - section S1](#). Control samples (samples with only contaminants and samples with only PA) were analyzed, and neither losses nor leaching of contaminants from microplastics was observed.

2.5. Desorption assessment

The contaminant-sorbed microplastics from the equilibrium point of the sorption experiments were used in the desorption assessment. For this, 1.5 mL of the contaminant solution were replaced by 1.5 mL of ultrapure water in the same tubes used in the sorption kinetics experiment. Then, these tubes were kept for 48 h (equilibrium time) on a roto torque shaker at 20 °C. All experiments were performed in triplicate. The sample preparation and chemical analysis were performed according to the procedures described in the previous section.

2.6. Sorption kinetic and isotherm models

The amount of contaminant sorbed at time t (q_t) in mg g⁻¹ was calculated by [eq. \(1\)](#), where C_0 is the contaminant initial concentration in solution (mg L⁻¹), C_t is the contaminant concentration in solution at time t (mg L⁻¹), V is the volume of contaminant solution (L), and m is the mass of PA microplastics (g).

$$q_t = \frac{(C_0 - C_t)V}{m} \quad (1)$$

The sorption efficiency (%) was obtained from the ratio between the amount of contaminant sorbed at time t and the contaminant initial concentration. The pseudo-1st-order (PFO) and pseudo-2nd-order (PSO) kinetic models were used in this study to evaluate the sorption mechanism of contaminants on PA microplastics.

The relationship between the amount of contaminant sorbed at equilibrium and the contaminant concentration in solution could be determined by sorption isotherms. The Langmuir and Freundlich isotherm models were used to explain the interaction between contaminants and microplastics. The mathematical expressions for the kinetic and isotherm models are shown in [Table S5](#).

2.7. Statistical analysis

All statistical tests were performed in Action Stat Version 3.7. Two-way analysis of variance (ANOVA) was used to evaluate significant differences in sorption efficiencies between four aquatic matrices for each contaminant. Tukey's test was used to assess significant differences among different groups. Probability levels ($p < 0.05$) were considered statistically significant.

2.8. Molecular dynamics and density functional theory (DFT) calculations

Classical molecular dynamics (MD) simulations were carried out to deeper investigate the sorption process of the three contaminants (ATZ, PGT, and TTR) onto PA (Nylon 6) microplastic surface. All simulations

were performed with the GROMACS 5.1.5 package ([Abraham et al., 2015](#), [van der Spoel et al., 2005](#)) to address the molecular conformations. The technical details are given in the **Supporting Information – section S2**. The simulations start with a system energy minimization step in the NVE ensemble, where number of particles (N), volume (V) and energy (E) are kept constants. The second step consists of the production by 30 ns in the NVT ensemble, where N, V and the set temperature (T) of 300 K are kept constant. The production step yields a trajectory with 30,000 configurations of the system. From MD production trajectory, 32 statistically uncorrelated configurations, evenly spaced i.e., one for every 938 configurations, were selected to calculate the solvation and sorption average energies through quantum single point calculations.

3. Results and discussion

3.1. Polyamide microplastic characterization

[Fig. S1a](#) shows the SEM image of PA microplastics. Irregular shapes and heterogeneous surfaces were observed in the microplastic particles, probably due to the milling process. The ATR-FTIR spectrum of microplastics ([Fig. S1b](#)) shows the fingerprint functional groups of PA with Pearson's r equal to 0.96 according to Open Specy ([Cowger et al., 2021](#); [Primpke et al., 2018](#)).

3.2. Aquatic matrices characterization

All aquatic matrices used in the sorption experiments were characterized in terms of target contaminant concentrations, pH, and conductivity, as shown in [Table S6](#). TTR and PGT were not found in any water sample. On the other hand, ATZ has been considered ubiquitous in the environment. Thus, ATZ concentrations ranged from 2.5 ng L⁻¹ to 42 ng L⁻¹ in GW, SFW, and SW. However, these concentrations are insignificant, approximately 20 thousand times lower than those used in the sorption experiments. The pH values ranged from 6.9 to 8.4, where the most neutral pH was observed in UW. The pH of the aquatic matrices could interfere with the sorption efficiency, especially for ATZ because this contaminant is a base herbicide, i.e., when the system pH is lower than its pK_a (1.7), the ATZ could form ions with a positive charge. So, this charge could affect the electrostatic interactions with PA. However, in the environment, the water systems' pH always is above the ATZ pK_a . The conductivity ranged from 0.06 µS cm⁻¹ to 11.64 mS cm⁻¹. UW presented a conductivity approximately 100-fold lower than GW and SFW, and both were around 100 times lower than SW. Like pH, conductivity could affect the interactions between microplastics and contaminants, as will be discussed later in section [3.5](#).

3.3. Sorption kinetic

The amount of ATZ, TTR, and PGT sorbed by PA microplastics (q_t) as a function of their contact times are shown in [Fig. 1](#). The kinetic studies demonstrated that the sorption occurs in the first hours of contact and a notable increase in q_t was observed until 12 h in the different aquatic matrices. The equilibrium was reached after 48 h since there were no significant changes in q_t for both contaminants until the final contact time (108 h). Therefore, for subsequent isotherm experiments, the equilibrium time was set as 48 h.

PFO and PSO models were fitted to experimental data, and their respective curves are shown in [Fig. 1](#). The theoretical parameters of each kinetic model are presented in [Table S7](#). The highest experimental q_e was observed for PGT (0.0833–0.0913 mg g⁻¹), followed by TTR (0.0535–0.0795 mg g⁻¹) and ATZ (0.0156–0.0256 mg g⁻¹) in all aquatic matrices. The sorption kinetics for the three contaminants were better fitted by the PSO model ($R^2 > 0.86$). In addition, this model presented lower q_e relative errors in GW, SFW, and SW matrices, ranging from 1.9% to -3.9% for ATZ, -1.0% to -5.8% for TTR, and 0.0% to -1.0%

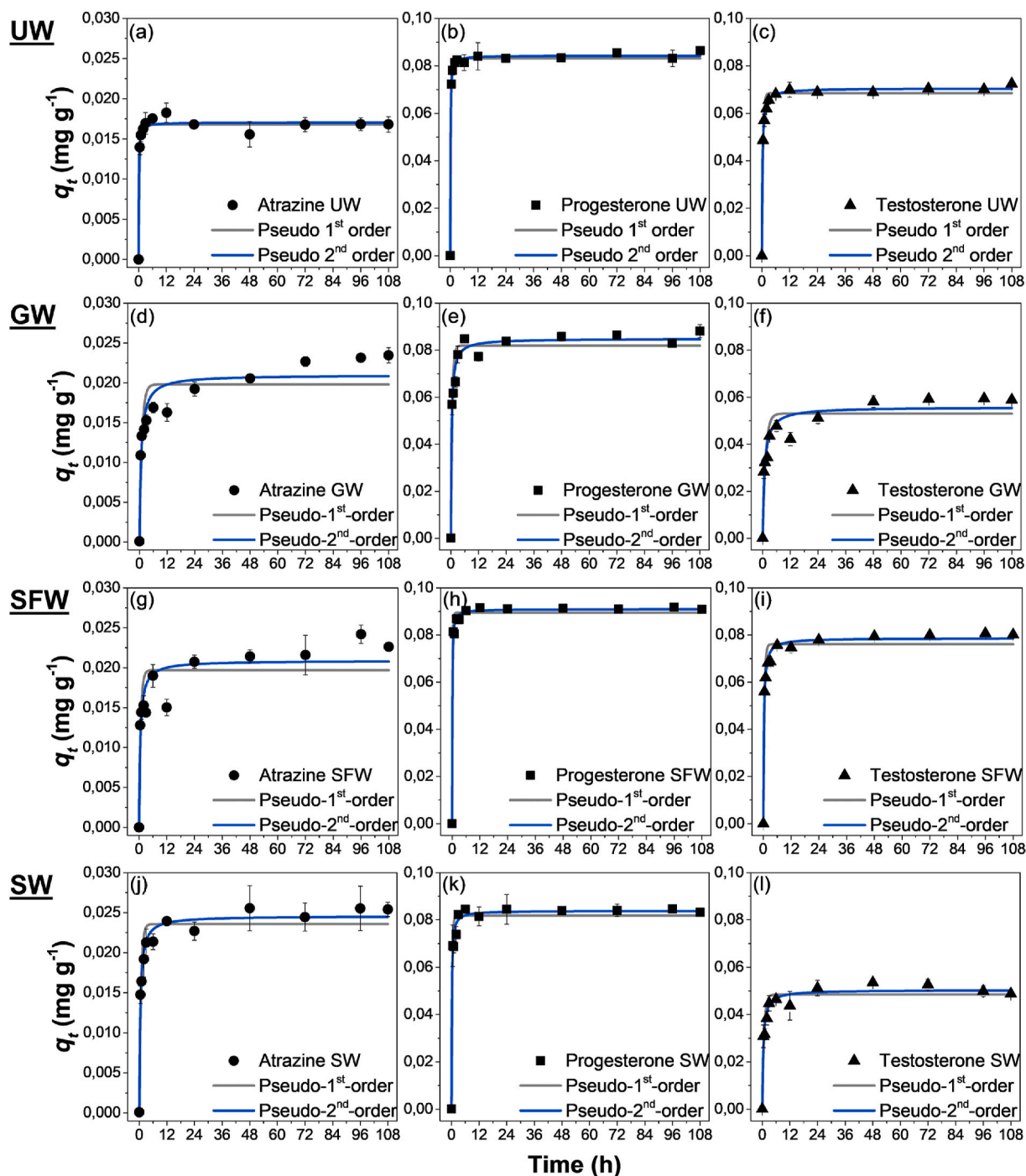


Fig. 1. Kinetic models for (a) Atrazine UW, (b) Progesterone UW, (c) Testosterone UW, (d) Atrazine GW, (e) Progesterone GW, (f) Testosterone GW, (g) Atrazine SFW, (h) Progesterone SFW, (i) Testosterone SFW, (j) Atrazine SW, (k) Progesterone SW, and (l) Testosterone SW. Experimental conditions: temperature = 20 °C; polyamide concentration = 10 g L⁻¹; contaminant concentration = 1 mg L⁻¹. UW = ultrapure water, GW = groundwater, SFW = surface water, SW = seawater.

for PGT.

PSO model has been used to describe the sorption of some hormones by microplastics, e.g., 17 α -ethynylestradiol, 17 β -estradiol, and estriol onto PA (Lara et al., 2021) and PGT onto polyethylene (PE), polystyrene (PS), and polypropylene (PP) (Siri et al., 2021). PSO model suggests that some events may be involved in the sorption process, such as surface sorption, mass transfer, and intraparticle diffusion. In addition, the model has been used to indicate chemisorption as a rate-limiting step; however, this is only an approximation because many other mechanisms are involved in sorption (Ma et al., 2019; Siri et al., 2021).

In general, ATZ sorption was faster than hormone sorption due to the

high values of k_2 (between 66 g mg⁻¹ h⁻¹ and 583 g mg⁻¹ h⁻¹). For example, in UW, ATZ presented a k_2 value around 4-fold higher than PGT and almost 10-fold higher than TTR, indicating that the equilibrium was reached more quickly. The same behavior was observed in GW and SW, with ATZ k_2 values higher than the other compounds. Only in SFW we observed that PGT presented higher k_2 (140 g mg⁻¹ h⁻¹) than the other two contaminants (ATZ = 92 g mg⁻¹ h⁻¹ and TTR = 52 g mg⁻¹ h⁻¹). It is worth mentioning that a comparing kinetic parameter, such as q_e and k_2 between different experiments becomes challenging due to the lack of standard protocol for experiments. Sorption studies with microplastics involve numerous aspects which are dependent on the

polymer (particle size, degradation stage, additives, concentration, molecular structure), the contaminant (concentration, physicochemical properties), and the environment (pH, ionic strength, organic matter content), among others. So, qualitatively, our results showed that the ATZ and PGT sorption on PA was faster when compared to other studies also fitted by PSO models. For instance, Zhao et al. (2020) verified that ATZ sorption was faster in polyurethane-PU ($k_2 = 2.16 \text{ g mg}^{-1} \text{ h}^{-1}$), but the highest sorbed amount was found in polybutylene succinate-PBS (q_e

$= 0.485 \text{ mg g}^{-1}$) using an ATZ solution (5.0 mg L^{-1}) containing CaCl_2 (0.01 mol L^{-1}) and microplastics (10 g L^{-1}) with particle size between 150 and 200 μm . Also, Sun et al. (2022) using ATZ solution at 20 mg L^{-1} containing CaCl_2 (1.1 mg L^{-1}) and NaNO_3 (200 mg L^{-1}) noted that the faster sorption ($k_2 = 15.392 \text{ g mg}^{-1} \text{ h}^{-1}$) takes place on polyvinyl chloride-PVC at 200 g L^{-1} with particle size of 22.4 μm , but the sorption was higher on 15 μm PE microplastics ($q_e = 0.028 \text{ mg g}^{-1}$). Finally, Wang et al. (2022) found faster sorption on PS ($k_2 = 2.730 \text{ g mg}^{-1} \text{ h}^{-1}$)

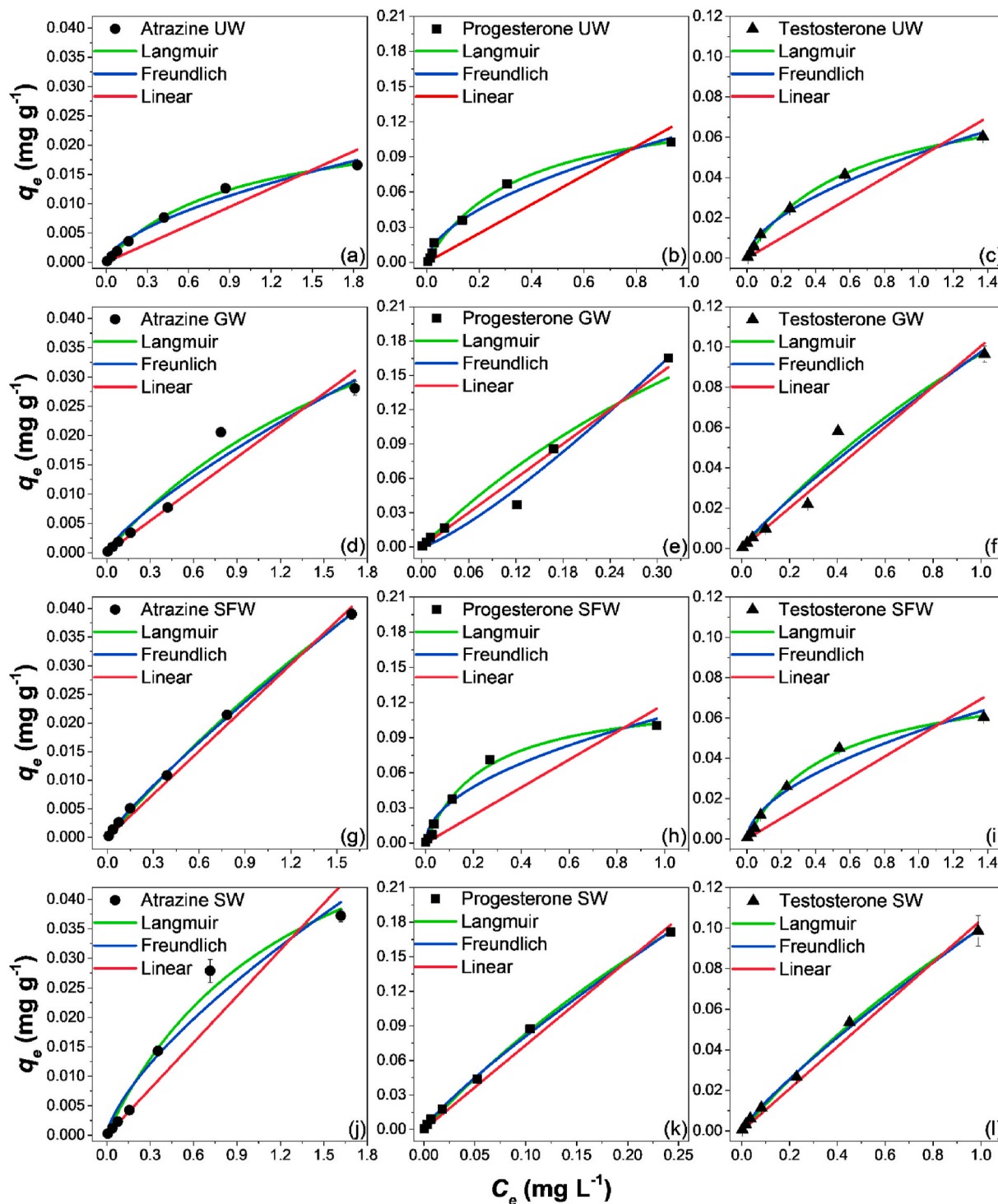


Fig. 2. Sorption isotherms for (a) Atrazine UW, (b) Progesterone UW, (c) Testosterone UW, (d) Atrazine GW, (e) Progesterone GW, (f) Testosterone GW, (g) Atrazine SFW, (h) Progesterone SFW, (i) Testosterone SFW, (j) Atrazine SW, (k) Progesterone SW, and (l) Testosterone SW. Experimental conditions: temperature = 20°C ; polyamide concentration = 10 g L^{-1} . UW = ultrapure water, GW = groundwater, SFW = surface water, SW = seawater.

than on same size PE and PP microplastics (178 μm) for a microplastics concentrations of 0.4 g L^{-1} and an ATZ concentration of 5.0 mg L^{-1} . Nonetheless, the interaction was more efficient between ATZ and PS ($q_e = 0.644 \text{ mg g}^{-1}$). For PGT, only one work reported that the sorption was faster on PP ($k_2 = 16.0 \text{ g mg}^{-1} \text{ h}^{-1}$) and higher on both PE and PS ($q_e = 0.3571 \text{ mg g}^{-1}$) (Siri et al., 2021). On the other hand, no comparison could be made for TTR sorption because, to the best of our knowledge, this is the first report of TTR sorption on microplastics.

3.4. Sorption isotherms

The Langmuir, Freundlich, and linear sorption isotherms were used to evaluate the concentration effect on the sorption efficiency at equilibrium. These isotherms are shown in Fig. 2 and their fitting parameters were summarized in Table S8. Langmuir ($0.9576 < R^2 < 0.9992$) and Freundlich ($0.9396 < R^2 < 0.9989$) models were better fitted than the linear model ($0.7164 < R^2 < 0.9931$). The K_L values ranged from 0.168 L mg^{-1} to 1.054 L mg^{-1} for ATZ, 0.355 L mg^{-1} to 2.045 L mg^{-1} for TTR, and 1.392 L mg^{-1} to 3.999 L mg^{-1} for PGT. The highest ATZ q_m (0.185 mg g^{-1}) was observed in SFW and maximum q_m values for TTR (0.380 mg g^{-1}) and PGT (0.675 mg g^{-1}) were obtained in SW.

The Langmuir isotherm showed a slight improvement in the R^2 values, indicating that the monolayer coverage could be a dominant process in the sorption of the three contaminants. Thus, Langmuir's model describes the physisorption process governed by electrostatic and hydrophobic interactions between the contaminants and PA particles, leading to the production of a monolayer coverage on the heterogeneous surface of the microplastics (Agboola and Benson, 2021; Al-Ghouti and Da'ana, 2020). Moreover, the sorption was a favorable process in all water matrices, according to the separation factor (R_L) values ($0 < R_L < 1$) obtained from Langmuir parameters (Al-Ghouti and Da'ana, 2020).

The partition coefficients (K_d) between the liquid phase (aquatic matrices) and the solid phase (PA microplastic) for each contaminant were obtained based on the linear model. The low sorption efficiency of ATZ on PA microplastics was reflected in the lowest K_d values, ranging from 0.010 L mg^{-1} to 0.026 L mg^{-1} . These values were higher than those found for other microplastics, such as PBS, polycaprolactone, and PU (Zhao et al., 2020), indicating that ATZ could interact with PA microplastics more efficiently. TTR and PGT presented K_d values between 0.050–0.104 L mg^{-1} and 0.119–0.733 L mg^{-1} , respectively. Thus, the average K_d values were positively correlated ($R^2 > 0.99$, see Fig. S2) with the octanol-water partition coefficients ($\log K_{OW}$), since the last also increase in the following order: ATZ < TTR < PGT.

3.5. Sorption efficiency

Sorption efficiencies in four different aquatic matrices at equilibrium (48 h) are shown in Fig. 3. PA microplastics presented the highest efficiency for PGT, followed by TTR and ATZ, in all matrices. The sorption efficiencies for ATZ were around 20% in all matrices. For TTR and PGT, the efficiencies were approximately 55–80% and 90%, respectively. ATZ sorption was investigated in other microplastics by Ateia et al. (2020), who observed sorptions higher than those found here, e.g., Nylon 1–70%, Nylon 66–90%, PE – 90%. As previously commented, it is evident that the experimental conditions could influence the contaminant sorbed amount.

As previously discussed, PGT has the highest $\log K_{OW}$, so, the PA sorption efficiencies are positively correlated to the contaminant hydrophobicity. This observation has been extensively discussed in the literature (Rai et al., 2022), so it is expected that contaminants with high K_{OW} tend to be more sorbed by microplastics. However, this is not a rule, and the opposite could be observed sometimes. For instance, Sleight et al. (2017) observed that phenanthrene does not have a stronger association with PVC microplastics than the 17 α -ethynylestradiol hormone, even though the first had the highest $\log K_{OW}$. The same behavior was observed by Fatema and Farenhorst (2022), who identified that

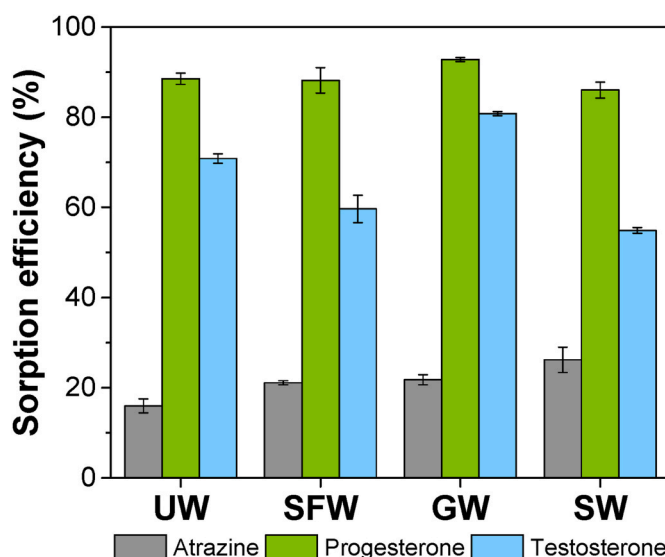


Fig. 3. Sorption efficiency for atrazine, progesterone, and testosterone in polyamide microplastics on ultrapure water (UW), surface water (SFW), groundwater (GW), and seawater (SW) at equilibrium time (48 h). Experimental conditions: temperature = 20 °C; polyamide concentration = 10 g L^{-1} ; contaminant concentration = 1 mg L^{-1} .

glyphosate ($\log K_{OW} = -3.20$) was more sorbed on PVC than the ATZ. This trend was also reported in polar PA microplastics in a study with three different hormones (estrone - $\log K_{OW} = 3.43$, 17 α -ethynylestradiol - $\log K_{OW} = 4.21$, and norethisterone - $\log K_{OW} = 2.99$). The estrone sorption was lower than the other two compounds, and this was attributed due to their different interactions, mainly the hydrogen bonds with PA microplastics (Hummel et al., 2021).

Significant differences (p -value < 0.05) were observed between sorption efficiencies for the three contaminants, showing that physicochemical properties of the system could interfere with their interaction with PA microplastic. PGT presented the highest interaction with PA microplastics (sorption efficiencies of at least 80%). Post-hoc analysis proved that sorption efficiencies for PGT were statistically different between SFW-SW and SFW-UW matrices. The lowest sorption efficiencies for PGT and TTR were observed in SW, which could be related to the higher concentration of salt ions when compared to the other matrices. Salt ions can occupy the sorption sites on the microplastic surface, promoting competitive sorption with contaminants. The Na^+ addition could affect the surface charge of the microplastics, decreasing the electrostatic interactions with the hormones (G. Liu et al., 2019; Upadhyay et al., 2022). Also, NaCl addition could promote an increase in the density and viscosity of the solution, which inhibits the mass transfer from the aqueous phase to the microplastic surface (salting-in effect) (G. Liu et al., 2019; Zhang et al., 2020). These phenomena have been shown in some studies with different microplastics, although it is highlighted that this could not be related only to the ionic strength but also to other variables, such as sorbent, sorbate, and electrolyte (Atugoda et al., 2020; Fu et al., 2021).

The opposite was observed for the ATZ sorption efficiencies due to the highest interaction occurring in SW. In this case, the increase in the sorption efficiency could be explained by the salting-out effect. Organic compounds may have their solubilities decreased in solution due to salt ions' presence, allowing for more interactions with the microplastic surface and contaminant. This agrees with the results reported by Wang et al. (2022), who observed a significant increase in ATZ sorption on PS, PP, and PE microplastics when the NaCl concentration was 1%.

The lowest sorption efficiency for ATZ was found in UW, and Tukey-test showed that ATZ sorption was statistically different between GW-SW, GW-UW, UW-SFW, and UW-SW matrices. No significant

differences in ATZ sorbed fractions on PE and PS microplastics were observed at three pH values (4, 7, and 10), according to Seidensticker et al. (2018). Recently, Wang et al. (2022) showed opposite results, concluding that the pH is a determining factor in the sorption process. They evaluated the ATZ sorption on PS, PE, and PP at eight pH values, and a higher sorption efficiency at neutral pH was observed. In the present study, all the pH values of the matrices were above ATZ pKa value. Thus, ATZ was mainly in its neutral form suggesting that sorption on microplastics could originate from interactions between the -NH groups of PA and the N-heteroaromatic ring or -NH groups of ATZ (Ateia et al., 2020; Zhao et al., 2020). Post-hoc analysis showed that TTR sorption was significantly different in all groups, meaning that any factors, such as polymer and contaminants properties and the environment characteristics, can affect sorption efficiency.

3.6. Desorption assessment

The desorption behavior in UW was evaluated to investigate the preference of three contaminants between the aquatic matrices and PA microplastic surface. Based on the previously equilibrium time (48 h) determined in the sorption kinetic analysis, the same contaminated microplastic samples were used to analyze the desorption. The sorption and desorption data are shown in Fig. 4. Only for ATZ, the desorption efficiency (~65%) was higher than sorption efficiency (~16%), showing its preference for being solubilized in water. However, the opposite was noted for TTR and PGT, which presented desorption efficiencies around 25% and 11%, respectively. Similar results for PGT desorption from PE (~30%) and PP (~30%) microplastics were obtained by Siri et al. (2021), who investigated the desorption in SFW and biological fluids. Also, the lower desorption rates for TTR and PGT could be attributed to the higher number of hydrogen bonds with the PA microplastics than ATZ, as will be shown in the next section. A similar observation was reported by Liu et al. (2019), who investigated the desorption rate of bisphenol A in 12 types of microplastics. They highlighted that no bisphenol A desorption was noted in PA due to the irreversible sorption process with strong hydrogen bonds.

The bioavailability of contaminants can be influenced by sorption/desorption mechanism onto microplastics. For instance, Sleight et al. (2017) demonstrated that the bioavailability of phenanthrene and 17 α -ethinylestradiol was reduced by 33% and 48%, respectively when these compounds were sorbed to PVC microplastics. On the other hand,

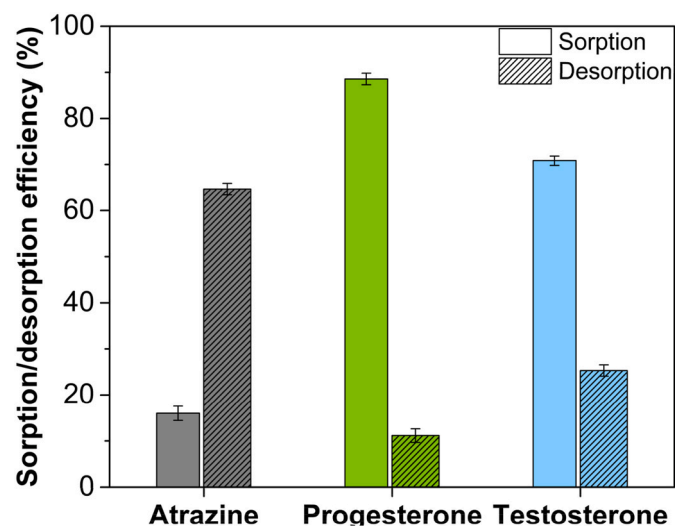


Fig. 4. Sorption and desorption efficiency for atrazine, progesterone, and testosterone on/from polyamide microplastics in ultrapure water at equilibrium (48 h). Experimental conditions: temperature = 20 °C; polyamide concentration = 10 g L⁻¹.

desorption of contaminants from microplastics under different physicochemical conditions within the gastrointestinal tract can increase the bioavailability causing severe damage to the biota, even in low concentrations (ng L⁻¹) (Guedes-Alonso et al., 2021).

3.7. Sorption energies and intermolecular interactions

Through simulations it was possible to sample different conformations of the system and probe the interactions between contaminants and the surface of PA particles. As defined in eq. S1, the E^{sol} represents the transfer energy of the contaminant from the solvent network to the microplastic surface, i.e., the lower the energy, the more easily the contaminant sorbs into the microplastic. The calculated average energies are given in Table S4. The sorption energy results indicated that PGT (12–15 kcal mol⁻¹) is the contaminant that sorbs the most on the surface of the polymer, followed by TTR (13–16 kcal mol⁻¹), whereas ATZ (19–22 kcal mol⁻¹) is the one that sorbs the least, in excellent agreement with the experiment of sorption efficiency. In addition, the calculated ΔE^{sol} values predict the higher experimental solubility of ATZ (33 mg L⁻¹) in water compared to PGT (8.8 mg L⁻¹) and TTR (23.4 mg L⁻¹) (NCBI, 2022).

The MD simulations revealed the specific interactions between contaminants and PA, which comprise mainly noncovalent interactions as hydrogen bonds (HB) and van der Waals (vdW) forces, as also reported by Xu et al. (2018) and Zhang et al. (2020) for sorption of sulfamethoxazole by PE microplastics and fluoroquinolones by PS nanoplastics. Some representative structures of simulated PA-contaminant complexes are displayed in Figs. 5 and 6 with intermolecular distances in the range of ≈ 1.7 –2.1 Å. The contaminant sorption seems to occur on the inner and outer surfaces of PA. Thus, Fig. 5a shows the ATZ inner sorption through vdW interactions between the -CH groups. Fig. 5b shows the ATZ both as N-H...N HB donor and acceptor, also via inner sorption. Meanwhile, Fig. 5c and Fig. 5d shows outer sorption through N-H...O HBs.

For TTR (49 atoms and a surface area of 338.683 Å²) and PGT (53 atoms and a surface area of 392.720 Å²), the sorption interaction takes place mostly at the outer surface of PA as shown in Fig. 6. It was observed that the interactions on the inner surface occur mainly by the nonpolar moieties through the vdW forces as shown in Fig. 6d and Fig. 6f. This may be related to the larger size of these molecules compared with ATZ (28 atoms and a surface area of 285.090 Å²), which leads to difficulty in penetration and stabilization onto inner surface.

The sorption mechanism occurs mainly via HBs between contaminant and PA surface. Then, to investigate the differences of the amount of sorption of the three investigated compounds, the number of HB-interacting configurations during the simulations was probed. In Fig. S3 we can observe that the sampled configurations of PA-contaminant complex mostly present only one HB, and that the ATZ interacts less with PA particles compared to the other contaminants. Otherwise, the PGT is the most interacting compound and as expected, only as an HB acceptor. It is interesting to note in Fig. S3 that although the TTR presents a hydroxyl group, it interacts mostly as an HB acceptor. Therefore, these results show that the higher sorption of PGT is driven by its stabilization via N-H...O HBs on the polymer surface. Furthermore, this corroborates to explain the experimental results which indicated a physisorption mechanism given by Langmuir's isotherm.

From the molecular point of view, the sorption efficiency and the co-transport across the aqueous solution can be rationalized in terms of polarity and basicity of contaminants and polymer molecules. For instance, the dipole moment of the PGT, ATZ, TTR, and PA is approximately 2.56 D, 4.34 D, 4.78 D, and 4.20 D, respectively, which is much higher compared with the dipole of water (~ 1.85 D) (Lide, 2004). Then, both the contaminants and polymer can easily solubilize and disperse in water. Although it has a smaller dipole, the solubility of the ATZ (33 mg L⁻¹) is higher than TTR (23.4 mg L⁻¹) because of the basicity of its

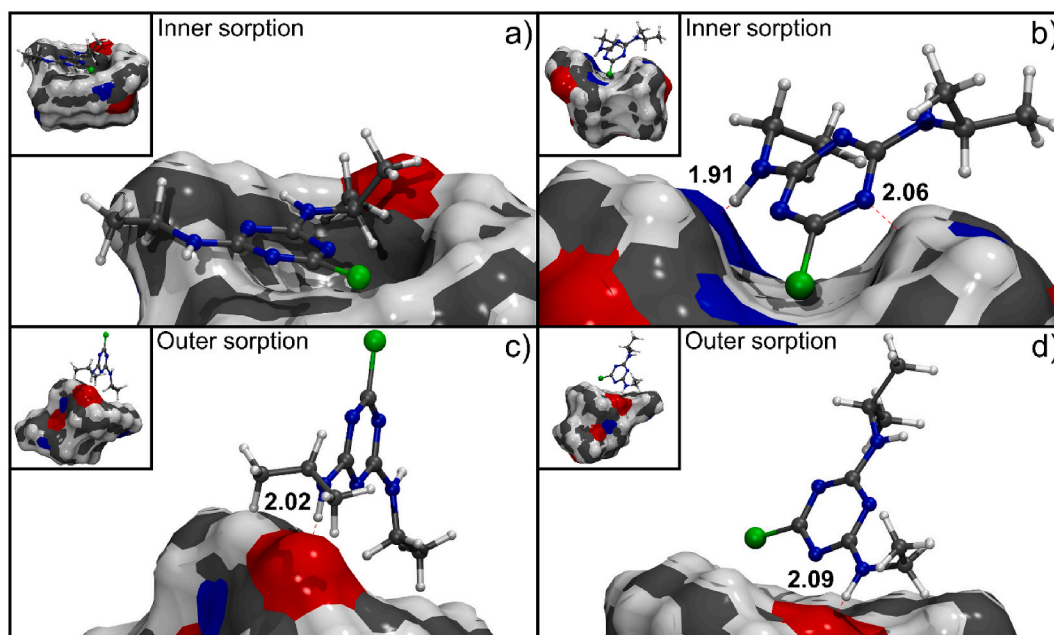


Fig. 5. Molecular dynamics configurations showing the main sorption mechanism interactions of ATZ onto PA microplastic surface: (a) electrostatic interactions between $-CH$ groups, (b) ATZ both as $N-H\cdots N$ hydrogen bond donor and acceptor, (c, d) ATZ as $N-H\cdots O$ hydrogen bond donor. The values in the figures are the hydrogen bond lengths in Å. Oxygen, nitrogen, carbon, hydrogen, and chlorine atoms are represented by red, blue, gray, white, and green colors, respectively.

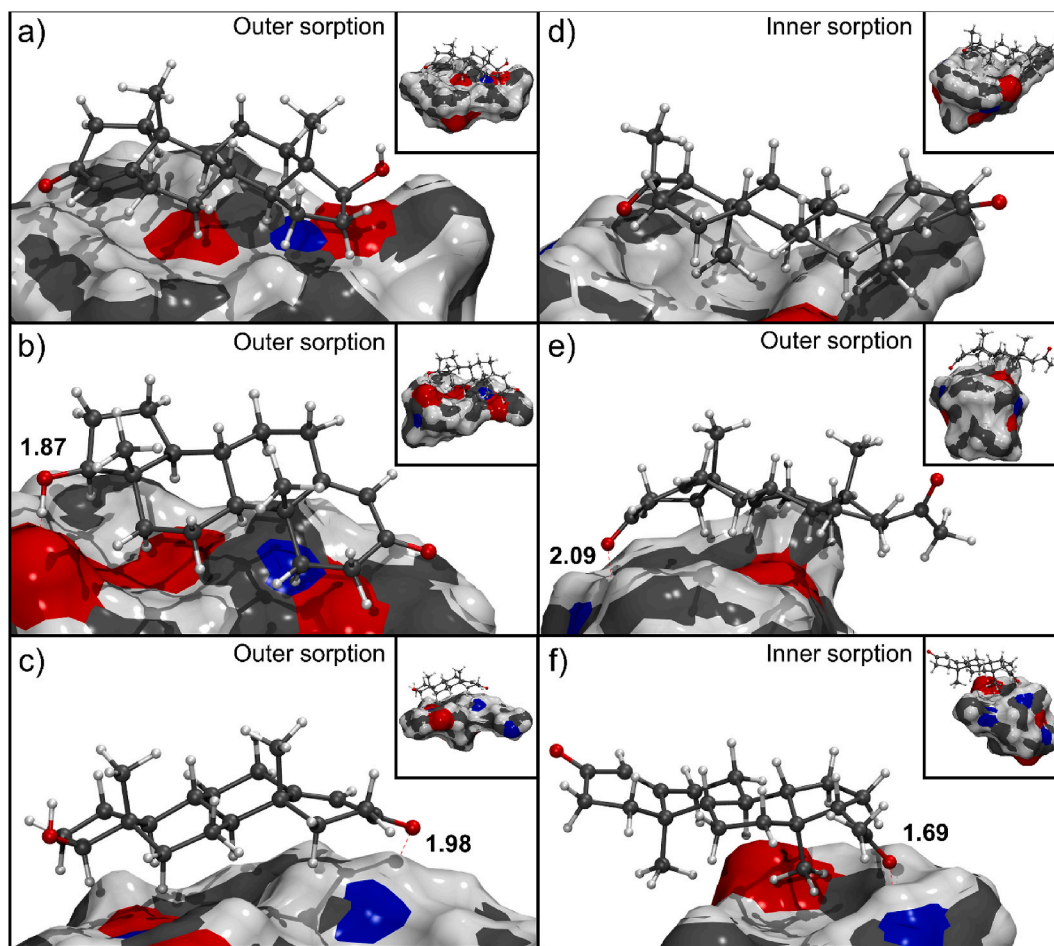


Fig. 6. Molecular dynamics configurations showing the main sorption mechanism interactions of the (a–c) TTR and (d–f) PGT onto PA microplastic surface: (a, d) electrostatic interactions between $-CH$ groups, (b) TTR as $O-H\cdots O$ hydrogen bond donor, (c) TTR and (e, f) PGT as $N-H\cdots O$ hydrogen bond acceptor. The values in the figures are the hydrogen bond lengths in Å. Oxygen, nitrogen, carbon, and hydrogen atoms are represented by red, blue, gray, and white colors, respectively.

amino groups, that make it more efficiently stabilized by HBs in aqueous solution (Hall, 1957). On the other hand, PGT should have a similar solubility to TTR when comparing their solvation energy (ΔE^{sol}_v). However, the dipole moment of PGT is much smaller (~ 2.56 D), resulting in a lower solubility (8.8 mg L^{-1}) and consequently higher sorption. Furthermore, the averaged dipole moment of PA-contaminant complex shows an increase compared to dissociated PA-contaminant: 13.52 D for PA-ATZ; 11.57 D for PA-PGT; 11.32 D for PA-TTR, which increases the contaminant's mobility in water by co-transport (Barbosa et al., 2020; Sleight et al., 2017), as also showed for BPA sorbed onto nanoplastics (Cortés-Arriagada, 2021) and pharmaceuticals/personal care products onto PS microplastics (Cortés-Arriagada et al., 2022).

4. Conclusions

For the first time, the sorption of a pesticide (ATZ) and two hormones (TTR and PGT) on PA microplastic was evaluated using theoretical and experimental design. It was evident that the water matrix in which sorption occurs is crucial to predict the behavior of contaminants in solution since significant differences ($p < 0.05$) were observed using four different aquatic matrices, UW, SW, SFW, and GW. PA microplastics presented the highest sorption efficiency for PGT ($\sim 90\%$), followed by TTR ($\sim 70\%$) and ATZ ($\sim 20\%$). In addition, desorption experiments in UW showed that ATZ displays higher affinity for water due to its high desorption efficiency. Kinetic studies showed that the PSO model fitted the experimental data best for all experiments, while Langmuir's model was the best isotherm to explain the concentration effect on sorption using an equilibrium time of 48 h. The experimental results were supported by theoretical calculations that showed high sorption energy for PGT. The calculations also suggest that the sorption mechanism is driven by HBs interactions and vdW forces, which characterized the physorption. We evaluate sorption/desorption rate of these three contaminants in a specific type of PA (Nylon 6 – Domamid H24). However, we understand that in the environment there are much more types of PA. The variations are related specially to the presence of chemical additives and morphology, which could influence in the microplastic sorption efficiency. Nevertheless, the amide group is common in all PA allowing the chemical interactions with ATZ, PGT and TTR be the same.

Microplastics are a real-worldwide issue, considering the actual plastic pollution scenario, especially in marine- and freshwater. Microscale studies are helpful to elucidate the transport of several species by microplastics in these environments. This work reveals that the differences in the chemical composition of aquatic matrices are crucial in the sorption capacity of microplastics. It is also observed that some species establish strong interactions with microplastics becoming a concern when these particles are ingested by biota and even humans. In this sense, considering the amount of plastic waste already spread in aquatic compartments and that around 12,000 Mt of plastic waste will be discharged into the environment by 2050 (Geyer et al., 2017), the contamination by microplastics themselves and with species-sorbed is enormous and could be made even worse. Thus, bioavailability and lixiviation studies coupled to chemical studies of the species associated with microplastics and their impacts mainly on aquatic organisms are essential.

Credit author statement

Mariana Dias: Methodology, Writing – original draft. **Patrick Batista and Lucas Ducati:** Theoretical methodology, Writing. **Cassiana Montagner:** Resources, Writing – review & editing, Funding acquisition.

Declaration of competing interest

The authors declare that they have no known competing financial interests or personal relationships that could have appeared to influence

the work reported in this paper.

Data availability

Data will be made available on request.

Acknowledgments

The authors thank the São Paulo Research Foundation (FAPESP) grants #2017/17750-3, #2018/07308-4, and #2018/21733-0 and #2020/10246-0 for financial support. The authors are also thankful to INCTAA (CNPq grants #573894/2008-6 and 465768/2014-8, and FAPESP grants #2008/57808-1 and #2014/50951-4). CCM thanks the CNPq grant #311422/2020-9. LCD also acknowledges the CNPq grant #306844/2020-6. The authors also thank Camila L. Madeira for contributions and English language improvement. This study was financed in part by the Coordenação de Aperfeiçoamento de Pessoal de Nível Superior-Brasil 2015/18790-3 (CAPES)-Finance Code 001.

Appendix B. Supplementary data

Supplementary data to this article can be found online at <https://doi.org/10.1016/j.chemosphere.2023.137949>.

Appendix A. Supporting Information

Chemical analysis; computational details; sorption and kinetic model expressions; aquatic matrices characterization; kinetic and isotherm parameters; energies of the PA-contaminant complexes; microplastic characterization; K_{OW} and K_d relationship; hydrogen bond interaction analysis.

References

- Abraham, M.J., Murtola, T., Schulz, R., Páll, S., Smith, J.C., Hess, B., Lindahl, E., 2015. GROMACS: high performance molecular simulations through multi-level parallelism from laptops to supercomputers. Software 1–2, 19–25. <https://doi.org/10.1016/j.softx.2015.06.001>.
- Adeel, M., Song, X., Wang, Y., Francis, D., Yang, Y., 2017. Environmental impact of estrogens on human, animal and plant life: a critical review. Environ. Int. 99, 107–119. <https://doi.org/10.1016/j.envint.2016.12.010>.
- Agboola, O.D., Benson, N.U., 2021. Physorption and chemisorption mechanisms influencing micro (nano) plastics-organic chemical contaminants interactions: a review. Front. Environ. Sci. 9, 1–27. <https://doi.org/10.3389/fenvs.2021.678574>.
- Al-Ghouti, M.A., Da'ana, D.A., 2020. Guidelines for the use and interpretation of adsorption isotherm models: a review. J. Hazard Mater. 393, 122383 <https://doi.org/10.1016/j.jhazmat.2020.122383>.
- Alonso, L.L., Demetrio, P.M., Agustina Etchegoyen, M., Marino, D.J., 2018. Glyphosate and atrazine in rainfall and soils in agroproductive areas of the pampas region in Argentina. Sci. Total Environ. 645, 89–96. <https://doi.org/10.1016/j.scitotenv.2018.07.134>.
- Ateia, M., Zheng, T., Calace, S., Tharayil, N., Pilla, S., Karanfil, T., 2020. Sorption behavior of real microplastics (MPs): insights for organic micropollutants adsorption on a large set of well-characterized MPs. Sci. Total Environ. 720, 137634 <https://doi.org/10.1016/j.scitotenv.2020.137634>.
- Atugoda, T., Wijesekara, H., Werellagama, D.R.I.B., Jinadasa, K.B.S.N., Bolan, N.S., Vithanage, M., 2020. Adsorptive interaction of antibiotic ciprofloxacin on polyethylene microplastics: implications for vector transport in water. Environ. Technol. Innovat. 19, 100971 <https://doi.org/10.1016/j.eti.2020.100971>.
- Barbosa, F., Adeyemi, J.A., Bocato, M.Z., Comas, A., Campiglia, A., 2020. A critical viewpoint on current issues, limitations, and future research needs on micro- and nanoplastic studies: from the detection to the toxicological assessment. Environ. Res. 182, 109089 <https://doi.org/10.1016/j.envres.2019.109089>.
- Caruso, G., 2019. Microplastics as vectors of contaminants. Mar. Pollut. Bull. 146, 921–924. <https://doi.org/10.1016/j.marpolbul.2019.07.052>.
- Cortés-Arriagada, D., 2021. Elucidating the co-transport of bisphenol A with polyethylene terephthalate (PET) nanoplastics: a theoretical study of the adsorption mechanism. Environ. Pollut. 270, 116192 <https://doi.org/10.1016/j.envpol.2020.116192>.
- Cortés-Arriagada, D., Miranda-Rojas, S., Camarada, M.B., Ortega, D.E., Alarcón-Palacio, V.B., 2022. The interaction mechanism of polystyrene microplastics with pharmaceuticals and personal care products. Sci. Total Environ. 160632 <https://doi.org/10.1016/j.scitotenv.2022.160632>.
- Cowger, W., Steinmetz, Z., Gray, A., Munno, K., Lynch, J., Hapich, H., Primpke, S., de Frond, H., Rochman, C., Herodotou, O., 2021. Microplastic spectral classification

- needs an open source community: open specy to the rescue. *Anal. Chem.* 93, 7543–7548. <https://doi.org/10.1021/acs.analchem.1c00123>.
- de Falco, F., di Pace, E., Cocca, M., Avella, M., 2019. The contribution of washing processes of synthetic clothes to microplastic pollution. *Sci. Rep.* 9, 1–11. <https://doi.org/10.1038/s41598-019-43023-x>.
- Dias, M.A., dos Santos, J.M., Pignati, W.A., Felix, E.P., 2021. Quantification and risk assessment of pesticides in southern Brazilian air samples using low-volume sampling and rapid ultrasound-assisted extraction. *Environ. Sci. Process Impacts* 23, 467–479. <https://doi.org/10.1039/D0EM00467G>.
- Fatema, M., Farenhorst, A., 2022. Sorption of pesticides by microplastics, charcoal, ash, and river sediments. *J. Soils Sediments* 22, 1876–1884. <https://doi.org/10.1007/s11368-022-03218-8>.
- Fu, L., Li, J., Wang, G., Luan, Y., Dai, W., 2021. Adsorption behavior of organic pollutants on microplastics. *Ecotoxicol. Environ. Saf.* 217, 112207 <https://doi.org/10.1016/j.ecoenv.2021.112207>.
- Geyer, R., Jambeck, J.R., Law, K.L., 2017. Production, use, and fate of all plastics ever made. *Sci. Adv.* 3, 25–29. <https://doi.org/10.1126/sciadv.1700782>.
- Guedes-Alonso, R., Sosa-Ferrera, Z., Santana-Rodríguez, J.J., 2021. Analysis of microplastics-sorbed endocrine-disrupting compounds in pellets and microplastic fragments from beaches. *Microchem. J.* 171, 106834 <https://doi.org/10.1016/j.microc.2021.106834>.
- Guo, X., Chen, C., Wang, J., 2019a. Sorption of sulfamethoxazole onto six types of microplastics. *Chemosphere* 228, 300–308. <https://doi.org/10.1016/j.chemosphere.2019.04.155>.
- Guo, X., Liu, Y., Wang, J., 2019b. Sorption of sulfamethazine onto different types of microplastics: a combined experimental and molecular dynamics simulation study. *Mar. Pollut. Bull.* 145, 547–554. <https://doi.org/10.1016/j.marpolbul.2019.06.063>.
- Hall, H.K., 1957. Correlation of the base strengths of amines I. *J. Am. Chem. Soc.* 79, 5441–5444. <https://doi.org/10.1021/ja01577a030>.
- Herzke, D., Ghaffari, P., Sundet, J.H., Tranang, C.A., Halsband, C., 2021. Microplastic fiber emissions from wastewater effluents: abundance, transport behavior and exposure risk for biota in an arctic fjord. *Front. Environ. Sci.* 9, 1–14. <https://doi.org/10.3389/fenvs.2021.662168>.
- Hummel, D., Fath, A., Hofmann, T., Hüffer, T., 2021. Additives and polymer composition influence the interaction of microplastics with xenobiotics. *Environ. Chem.* 18, 101. <https://doi.org/10.1071/EN21030>.
- IBAMA, 2020. Brazilian Institute of Environment and Renewable Natural Resources. Boletins anuais de produção, importação, exportação e vendas de agrotóxicos no Brasil.
- ISO, 2020. ISO/TR 21960:2020 Plastics - Environmental Aspects - State of Knowledge and Methodologies.
- Lara, L.Z., Bertoldi, C., Alves, N.M., Fernandes, A.N., 2021. Sorption of endocrine disrupting compounds onto polyamide microplastics under different environmental conditions: behaviour and mechanism. *Sci. Total Environ.* 796, 148983 <https://doi.org/10.1016/j.scitotenv.2021.148983>.
- Li, J., Zhang, K., Zhang, H., 2018. Adsorption of antibiotics on microplastics. *Environ. Pollut.* 237, 460–467. <https://doi.org/10.1016/j.envpol.2018.02.050>.
- Li, Y., Lu, Z., Abrahamsson, D.P., Song, W., Yang, C., Huang, Q., Wang, J., 2021. Non-targeted analysis for organic components of microplastic leachates. *Sci. Total Environ.* 151598 <https://doi.org/10.1016/j.scitotenv.2021.151598>.
- Lide, D.R., 2004. CRC Handbook of Chemistry and Physics, vol. 85. CRC Press.
- Liu, G., Zhu, Z., Yang, Y., Sun, Y., Yu, F., Ma, J., 2019. Sorption behavior and mechanism of hydrophilic organic chemicals to virgin and aged microplastics in freshwater and seawater. *Environ. Pollut.* 246, 26–33. <https://doi.org/10.1016/j.envpol.2018.11.100>.
- Liu, X., Shi, H., Xie, B., Dionysiou, D.D., Zhao, Y., 2019. Microplastics as both a sink and a source of bisphenol A in the marine environment. *Environ. Sci. Technol.* 53, 10188–10196. <https://doi.org/10.1021/acs.est.9b02834>.
- Ma, J., Zhao, J., Zhu, Z., Li, L., Yu, F., 2019. Effect of microplastic size on the adsorption behavior and mechanism of triclosan on polyvinyl chloride. *Environ. Pollut.* 254, 113104 <https://doi.org/10.1016/j.envpol.2019.113104>.
- Montagner, C.C., Dias, M.A., Paiva, E.M., Vidal, C., 2021. Microplastics: Environmental occurrence and analytical challenges. *Quim. Nova* 44, 1328–1352. <https://doi.org/10.21577/0100-4042.20170791>.
- Montagner, C., Sodr , F., Acayaba, R., Vidal, C., Campestrini, I., Locatelli, M., Pescara, I., Albuquerque, A., Umbuzeiro, G., Jardim, W., 2018. Ten years-snapshot of the occurrence of emerging contaminants in drinking, surface and ground waters and wastewaters from S o Paulo state, Brazil. *J. Braz. Chem. Soc.* 30, 614–632. <https://doi.org/10.21577/0103-5053.20180232>.
- Montagner, C.C., Umbuzeiro, G.A., Pasquini, C., Jardim, W.F., 2014. Caffeine as an indicator of estrogenic activity in source water. *Environ. Sci.: Process. Impacts* 16, 1866–1869. <https://doi.org/10.1039/C4EM00058G>.
- NCBI, 2022. National Center for Biotechnology Information. PubChem Compound Database [WWW Document]. URL: <https://pubchem.ncbi.nlm.nih.gov/>. accessed 7.24.22.
- Primpke, S., Wirth, M., Lorenz, C., Gerds, G., 2018. Reference database design for the automated analysis of microplastic samples based on Fourier transform infrared (FTIR) spectroscopy. *Anal. Bioanal. Chem.* 410, 5131–5141. <https://doi.org/10.1007/s00216-018-1156-x>.
- Rai, P.K., Sonne, C., Brown, R.J.C., Younis, S.A., Kim, K.-H., 2022. Adsorption of environmental contaminants on micro- and nano-scale plastic polymers and the influence of weathering processes on their adsorptive attributes. *J. Hazard Mater.* 427, 127903 <https://doi.org/10.1016/j.jhazmat.2021.127903>.
- Richardson, S.D., Kimura, S.Y., 2016. Water analysis: emerging contaminants and current issues. *Anal. Chem.* 88, 546–582. <https://doi.org/10.1021/acs.analchem.5b04493>.
- Richardson, S.D., Ternes, T.A., 2022. Water analysis: emerging contaminants and current issues. *Anal. Chem.* 94, 382–416. <https://doi.org/10.1021/acs.analchem.1c04640>.
- Sadeghnia, H., Shahba, S., Ebrahimzadeh-Bideskan, A., Mohammadi, S., Malvandi, A.M., Mohammadipour, A., 2021. Atrazine neural and reproductive toxicity. *Toxin Rev.* 1–14. <https://doi.org/10.1080/15569543.2021.1966637>, 0.
- Sait, S.T.L., S rensen, L., Kubowicz, S., Vike-Jonas, K., Gonzalez, S.v., Asimakopoulos, A. G., Booth, A.M., 2021. Microplastic fibres from synthetic textiles: environmental degradation and additive chemical content. *Environ. Pollut.* 268, 115745 <https://doi.org/10.1016/j.envpol.2020.115745>.
- Seidensticker, S., Grathwohl, P., Lamprecht, J., Zarfl, C., 2018. A combined experimental and modeling study to evaluate pH-dependent sorption of polar and non-polar compounds to polyethylene and polystyrene microplastics. *Environ. Sci. Eur.* 30, 30. <https://doi.org/10.1186/s12302-018-0155-z>.
- Seidensticker, S., Zarfl, C., Cirpka, O.A., Grathwohl, P., 2019. Microplastic-contaminant interactions: influence of nonlinearity and coupled mass transfer. *Environ. Toxicol. Chem.* 38, 1635–1644. <https://doi.org/10.1002/etc.4447>.
- Siri, C., Liu, Y., Masset, T., Duf oi, W., Oldham, D., Minghetti, M., Grandjean, D., Breider, F., 2021. Adsorption of progesterone onto microplastics and its desorption in simulated gastric and intestinal fluids. *Environ. Sci. Process Impacts* 23, 1566–1577. <https://doi.org/10.1039/D1EM00226K>.
- Sleight, V.A., Bakir, A., Thompson, R.C., Henry, T.B., 2017. Assessment of microplastic-sorbed contaminant bioavailability through analysis of biomarker gene expression in larval zebrafish. *Mar. Pollut. Bull.* 116, 291–297. <https://doi.org/10.1016/j.marpolbul.2016.12.055>.
- Song, Xiaowei, Wu, X., Song, Xiaoping, Shi, C., Zhang, Z., 2021. Sorption and desorption of petroleum hydrocarbons on biodegradable and nondegradable microplastics. *Chemosphere* 273, 128553. <https://doi.org/10.1016/j.chemosphere.2020.128553>.
- Sousa, J.C.G., Ribeiro, A.R., Barbosa, M.O., Pereira, M.F.R., Silva, A.M.T., 2018. A review on environmental monitoring of water organic pollutants identified by EU guidelines. *J. Hazard Mater.* 344, 146–162. <https://doi.org/10.1016/j.jhazmat.2017.09.058>.
- Stefano, P.H.P., Roisenberg, A., Santos, M.R., Dias, M.A., Montagner, C.C., 2022. Unraveling the occurrence of contaminants of emerging concern in groundwater from urban setting: a combined multidisciplinary approach and self-organizing maps. *Chemosphere* 299, 134395. <https://doi.org/10.1016/j.chemosphere.2022.134395>.
- Sun, S., Sui, H., Xu, L., Zhang, J., Wang, D., Zhou, Z., 2022. Effect of freeze-thaw cycle aging and high-temperature oxidation aging on the sorption of atrazine by microplastics. *Environ. Pollut.* 307, 119434 <https://doi.org/10.1016/j.envpol.2022.119434>.
- Torres, F.G., Dioses-Salinas, D.C., Pizarro-Ortega, C.I., De-la-Torre, G.E., 2021. Sorption of chemical contaminants on degradable and non-degradable microplastics: recent progress and research trends. *Sci. Total Environ.* 757, 143875 <https://doi.org/10.1016/j.scitotenv.2020.143875>.
- Upadhyay, R., Singh, S., Kaur, G., 2022. Sorption of pharmaceuticals over microplastics' surfaces: interaction mechanisms and governing factors. *Environ. Monit. Assess.* 194, 803. <https://doi.org/10.1007/s10661-022-10475-0>.
- van der Spoel, D., Lindahl, E., Hess, B., Groenhof, G., Mark, A.E., Berendsen, H.J.C., 2005. GROMACS: fast, flexible, and free. *J. Comput. Chem.* 26, 1701–1718. <https://doi.org/10.1002/jcc.20291>.
- Wang, Y., Liu, C., Wang, F., Sun, Q., 2022. Behavior and mechanism of atrazine adsorption on pristine and aged microplastics in the aquatic environment: kinetic and thermodynamic studies. *Chemosphere* 292, 133425. <https://doi.org/10.1016/j.chemosphere.2021.133425>.
- Xu, B., Liu, F., Brookes, P.C., Xu, J., 2018. The sorption kinetics and isotherms of sulfamethoxazole with polyethylene microplastics. *Mar. Pollut. Bull.* 131, 191–196. <https://doi.org/10.1016/j.marpolbul.2018.04.027>.
- Zhang, H., Liu, F., Wang, S., Huang, T., Li, M., Zhu, Z., Liu, G., 2020. Sorption of fluoroquinolones to nanoplastics as affected by surface functionalization and solution chemistry. *Environ. Pollut.* 262, 114347 <https://doi.org/10.1016/j.envpol.2020.114347>.
- Zhao, L., Rong, L., Xu, J., Lian, J., Wang, L., Sun, H., 2020. Sorption of five organic compounds by polar and nonpolar microplastics. *Chemosphere* 257, 127206. <https://doi.org/10.1016/j.chemosphere.2020.127206>.